3.3 Strongly Correlated Quantum Systems

Theoretical study of strongly correlated electron systems using quantum many-body simulation and information science

Yukitoshi MOTOME
Department of Applied Physics,
The University of Tokyo, Bunkyo, Tokyo 113-8656

We have theoretically studied a variety of strongly-correlated electron systems by using numerical methods, including first-principles calculations, quantum many-body calculations, and machine learning (project numbers: 2024-Ca-0065 and 2024-Cb-0020). We also made several collaborations with experiments. During the last fiscal year, we have achieved substantial progress on the following topics.

(i) *Kitaev quantum spin liquids and Majorana fermions*: We clarified the origin of a chiral spin liquid state, which we discovered last year in the *S*=1 Kitaev model with bilinear-biquadratic interactions, by comparative studies of SU(3), O(3), and a discrete spin models [1]. We also studied effects of dissipation in the non-Hermitian Kitaev model under a magnetic field [2]. In addition, we demonstrated that rare-earth magnets can be good candidates for the Kitaev magnets [3,4]. Furthermore, we proposed new experimental platforms in heterostructures composed of van der Waals magnets [5] and ilmenite oxides [6]. Finally, we showed that the spin Seebeck effect can be a good probe of Majorana fermions in the Kitaev spin liquid [7]. The project leader gave a lecture in 物性若手夏の学校 on quantum spin liquids [8].

(ii) *Topological spin crystals and their dynamics*: Extending the research until the last years, we clarified how one-dimensional chiral solitons can penetrate into the system from the edges by using the Landau-Lifshitz-Gilbert dynamics [9]. We also unveiled a peculiar Hall response of magnetic torons — pairs of hedgehogs and antihedgehogs connected by skyrmion strings, whose Hall angle ranges from zero to infinity [10]. In addition, we proposed a stable superstructure made of magnetic hopfions — closed rings of twisted skyrmion tubes, by carefully investigating the interactions between magnetic hopfions [11].

(iii) *Topological phase transitions*: By using first-principles calculations, we showed that a monolayer of Co-based shandite exhibits topological transitions by rotating the magnetic field [12]. We also demonstrated that the Haldane model on a 1/6-depleted honeycomb lattice, which we call the Bishamon-kikkou lattice, and its connection to the honeycomb lattice exhibit peculiar topological insulating and metallic states and phase transitions between them [13].

(iv) *Collaborations with experimental groups*: We made fruitful collaborations on experiments for spin-polarized STM measurements of topological spin crystals in $GdRu_2Si_2$ [14], pressure-induced quantum melting of chiral spin order in FeGe [15], and anomalous Hall effects in a *p*-wave magnet with a helical magnetic order, $Gd_3Ru_4Al_{12}$ [16].

(v) *Development of new theoretical methods and their applications*: We proposed a new framework, which we call "physical reservoir probing", inversely exploiting the framework of quantum reservoir computing [17]. We demonstrate that this framework is powerful to identify quantum critical points in a wide range of quantum phase transitions, even for topological ones [18]. We also applied the inverse Hamiltonian design that we developed to discover new Hamiltonians with maximized quantum entanglement [19].

References

[1] R. Pohle, N. Shannon, and Y. Motome, Phys. Rev. Research **6**, 033077 (2024).

[2] K. Fukui, Y. Kato, and Y. Motome, Phys. Rev. B **110**, 024429 (2024).

[3] S.-H. Jang and Y. Motome, Commun. Mater. **5**, 192 (2024).

[4] S.-H. Jang and Y. Motome, Phys. Rev. B **110**, 155124 (2024).

[5] L. Zhang and Y. Motome, Phys. Rev. B **110**, L241109 (2024).

[6] Y.-F. Zhao, S.-H. Jang, and Y. Motome, preprint (arXiv:2403.09112).

[7] Y. Kato, J. Nasu, M. Sato, T. Okubo, T. Misawa, and Y. Motome, Phys. Rev. X **15**, 011050 (2025).

[8] 求 幸年:第 69 回物性若手夏の学校 講義「スピン液体の物理」.

[9] K. Shimizu, S. Okumura, Y. Kato, and Y. Motome, Phys. Rev. B **111**, 024411 (2025).

[10] K. Shimizu, S. Okumura, Y. Kato, and Y. Motome, Commun. Phys. **8**, 69 (2025).

[11] S. Kasai, K. Shimizu, S. Okumura, Y. Kato, and Y. Motome, preprint (arXiv:2411.00396).

[12] K. Nakazawa, Y. Kato, and Y. Motome, Phys. Rev. B **110**, 085112 (2024).

[13] S. Ikegami, K. Fukui, S. Okumura, Y. Kato, and Y. Motome, Phys. Rev. B **110**, 245107 (2024).

[14] J. Spethmann, Y. Motome *et al.*, Phys. Rev. Materials **8**, 064404 (2024).

[15] Y. Fujishiro, K. Nakazawa, Y. Kato, Y. Motome *et al.*, Phys. Rev. B **110**, L220401 (2024).

[16] R. Yamada, S. Okumura, Y. Motome *et al.*, preprint (arXiv:2502.10386).

[17] K. Kobayashi and Y. Motome, preprint (arXiv:2308.00898).

[18] K. Kobayashi and Y. Motome, preprint (arXiv:2402.07097), to be published in Nat. Commun.

[19] K. Inui and Y. Motome, Phys. Rev. Research **6**, 033080 (2024).

Development of Transformer+PP Wave Function

Yusuke NOMURA

Institute for Materials Research (IMR), Tohoku University,
2-1-1 Katahira, Aoba-ku, Sendai 980-8577

Analyzing quantum many-body problems is one of the central challenges in condensed matter physics. In recent years, there has been a growing interest in utilizing the expressive power of artificial neural networks to approximate quantum many-body wave functions. This line of research began with the seminal work by Carleo and Troyer in 2017, where a restricted Boltzmann machine (RBM) was introduced to represent quantum states [1].

Since then, a variety of neural network architectures have been explored for quantum-state representation. Notably, a transformer-based wave function was recently proposed by Viteritti *et al*., demonstrating high accuracy in capturing ground states of quantum spin systems [2].

The most challenging applications, however, lie in strongly correlated electron (fermionic) systems [3], which serve as a rich platform for exotic phenomena such as high-temperature superconductivity. To apply neural-network wave functions to fermionic systems, it is essential to satisfy the anti-commutation relations inherent to fermions.

One established approach is to combine a symmetric neural network-based wave function with an antisymmetric fermionic wave function, such as a Slater determinant. For example, the RBM combined with a pair-product (PP) wave function has achieved state-of-the-art accuracy in simulating the two-dimensional Hubbard model [4].

Building on this foundation, we are now exploring the combination of transformer-based wave functions with the PP wave function. Given the greater flexibility of transformers compared to RBMs, we expect the transformer+PP wave function to outperform the RBM+PP in terms of accuracy.

We have completed the implementation of a vision transformer for quantum spin systems, along with an efficient parameter-update scheme known as minSR [5]. We are now in the final stages of integrating the vision transformer with the PP wave function, which is an important next step that we aim to complete in the near future.

References

[1] G. Carleo and M. Troyer, Science **355**, 602 (2017).

[2] L. Viteritti *et al*., Phys. Rev. Lett. **130**, 236401 (2023).

[3] D. Wu *et al*., Science **386**, 296 (2024).
[4] Y. Nomura, A. S. Darmawan, Y. Yamaji, and M. Imada, Phys. Rev. B **96**, 205152 (2017).
[5] A. Chen and M. Heyl, Nat. Phys., **20**, 1476 (2024).

Studies on Quantum Many-Body Problem by Machine Learning

Masatoshi IMADA
Physica Division, Department of Engineering and Applied Sciences, Sophia University, 7-1 Kioi-cho, Chiyoda-ku Tokyo, 102-8554

Numerical method to construct ground-state wave functions of strongly interacting quantum many-body systems is one of the grand challenges in physics. Various algorithms have been proposed. Recently, neural network with Boltzmann machine has established an accurate way to approximate ground states of quantum spin systems [1] as well as itinerant fermion systems [2]. These neural networks are constructed by introducing hidden variables that are described by classical degrees of freedom.

In this project, we have explored mapping of the Hubbard model (in general, interacting lattice fermions) to noninteracting multi-component fermion models in the ground states, from which we have proposed a quantum machine learning algorithm called Fermi machine aiming at an efficient quantum many-body solver [3]. Fermion systems are introduced as the hidden part coupled to the physical system, instead of the classical one such as the Ising spins in the previous neural networks. This algorithm has been designed stimulated by the successful descriptions of strongly correlated electron systems by fractionalized fermions [4, 5]. After showing the exact correspondences of 1- and 2-site Hubbard models to two-component noninteracting fermions, a numerical algorithm of the quantum machine learning for the Hubbard model was proposed. Benchmark for the 4-site systems was successfully presented.

In the conventional variational Monte Carlo method, the fermion Slater determinant or Pfaffian is used as the starting point [6]. A crucial difference of the present Fermi machine is the entanglement with the hidden fermion degrees of freedom hybridizing with the physical (visible) fermions in the physical Hubbard model, which allows the formation of the gap structure in the spectra without spontaneous symmetry breaking, generating zeros of the Green's functions as well as poles as in the case of the genuine Mott insulator.

The project was financially supported by MEXT KAKENHI, Transformative Research Area (Grant No. JP22H05111 and No. JP22H05114). and also supported by MEXT under the grant number JPMXP1020230411.

References

[1] G. Carleo and M. Troyer, Science **355**, 602 (2017).

[2] Y. Nomura, A. S. Darmawan, Y. Yamaji, and M. Imada, Phys. Rev. B **96**, 205152 (2017).

[3] M. Imada. J. Phys. Soc. Jpn. **93**, 104002 (2024).

[4] S. Sakai, M. Civelli, and M. Imada, Phys. Rev. Lett. **116**, 057003 (2016).

[5] M. Imada: J. Phys. Soc. Jpn. **90** (2021) 111009.

[6] T. Misawa *et al.* Comput. Phys. Commun. **235**, 447 (2019).

Massively parallel variational Monte Carlo method for excitation spectra augmented by artificial neural networks

Youhei YAMAJI
Research Center for Materials Nanoarchitectonics, National Institute for Materials Science
Namiki, Tsukuba-shi, Ibaraki 305-0044

We have extended the dynamical variational Monte Carlo (dVMC) method [1, 2] for dynamical structure factors to simulating photoemission/inverse photoemission and resonant inelastic x-ray scattering spectra. In Fig. 1, the charge and spin dynamical structure factors (left panel) and momentum resolved inverse photoemission spectrum (right panel) for a one-dimensional half-filled Hubbard model are shown as examples of the extended dVMC results. By combining the results of the dynamical structure factors and the inverse photoemission, we can obtain the resonant inelastic x-ray scattering spectrum as well.

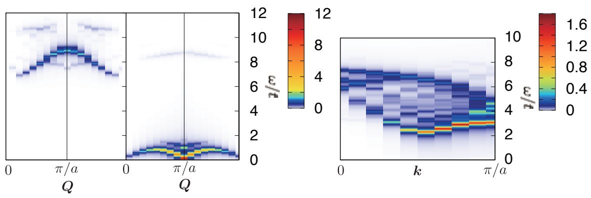

Figure 1: Examples of dVMC results for the one-dimensional Hubbard model at half-filling with 18 sites.

In the present project, we have introduced the quantum number projections [3] omitted in the previous version of the dVMC [2], to improve the accuracy and efficiency of the shared memory parallelization. To further improve the accuracy of the numerical spectroscopy realized by the dVMC method, we also incorporate the restricted Boltzmann machine, which was implemented in the original mVMC [4], and the feed-forward deep neural network, as a part of the generalized Jastrow-Gutzwiller correlation factor.

By further analyzing the resonant inelastic x-ray scattering simulation, we can identify the mutual correlations between single-particle spectral weight and charge and spin excitations. In the one-dimensional Hubbard model, for example, the correlations indeed enable us to identify the spinon and holon branches.

We will apply the method developed in the present project to the low-energy *ab initio* hamiltonians for the cuprate superconductors. To improve the parallelization efficiency of the present dVMC method, the population Monte Carlo that may shorten the warming up process will be useful.

References

[1] T. Li and F. Yang: Phys. Rev. B **81**, 214509 (2010).

[2] K. Ido, *et al.*: Phys. Rev. B **101**, 075124 (2020).

[3] T. Mizusaki and M. Imada: Phys. Rev. B **69**, 125110 (2004).

[4] T. Misawa, *et al.*: Comput. Phys. Commun. **235**, 447 (2019).

Generation of spin model based on machine learning

Satoru Hayami
Graduate School of Science, Hokkaido University, Sapporo 060-0810, Japan

Spin textures that exhibit fundamentally distinct physical properties from those of conventional ferromagnetic and antiferromagnetic systems have been the subject of extensive investigation in both theoretical and experimental contexts. Among these, the magnetic skyrmion, which is characterized by a swirling, topologically nontrivial spin configuration, has served as a focal point in the field of topological magnetism since its initial discovery in 2009. Although skyrmion crystal phases, comprising periodic arrays of magnetic skyrmions, have been experimentally realized in a variety of materials, the precise conditions under which such phases are stabilized, particularly with respect to lattice structures and magnetic interactions, remain to be fully understood. In the project with numbers 2024-Ca-0003 and 2024-Cb-0002, we have undertaken a series of numerical investigations aimed at elucidating the mechanisms responsible for the stabilization of magnetic skyrmion crystal phases under distinct situations. We have presented the main results this year below.

(i) Field-induced transformation between triangular and square skyrmion crystals in a tetragonal polar magnet: We have investigated magnetic field-induced transitions between triangular and square skyrmion crystals in a polar tetragonal magnet [1]. Using simulated annealing of a classical spin model, we have revealed that the competition between Dzyaloshinskii-Moriya and RKKY interactions at multiple wave vectors drives structural transitions in skyrmion lattices. The results demonstrate how magnetic frustration in momentum space can stabilize distinct skyrmion phases, such as distorted-triangular, square, and distorted-square types. These findings provide insight into topological phase transitions and may guide future exploration of skyrmion phenomena in noncentrosymmetric magnets.

(ii) Double-Q and quadruple-Q instabilities at low-symmetry ordering wave vectors under tetragonal symmetry: We have investigated the emergence of double-Q and quadruple-Q magnetic instabilities at low-symmetry wave vectors on a square lattice under tetragonal symmetry [2]. By employing simulated annealing for a classical spin model, we have classified four types of multiple-Q phases depending on the position of the ordering wave vectors. The results reveal that isotropic and anisotropic multiple-Q states can be stabilized without requiring Dzyaloshinskii-Moriya interactions. These findings highlight a novel route to realizing exotic, non-skyrmionic spin textures through momentum-space magnetic frustration.

(iii) Anisotropic skyrmion crystal on a centrosymmetric square lattice under an in-plane magnetic field: We have investigated the stabilization of skyrmion crystals on a centrosymmetric square lattice under an in-plane magnetic field [3]. By performing simulated annealing for an effective spin model, we have demonstrated that the interplay between easy-plane magnetic anisotropy, biquadratic interactions, and high-harmonic wave-vector interactions is essential for stabilizing anisotropic skyrmion crystals. The resulting skyrmion crystal features a vortex-antivortex pair with opposite out-of-plane spin polarizations. We

found that various double-Q phases also emerge, depending on magnetic field strength and anisotropy. These findings reveal new routes for realizing topological spin textures in centrosymmetric magnets with tunable anisotropy under an in-plane magnetic field.

(iv) XXZ-type interlayer exchange interaction in the bilayer triangular-lattice system as a source of multiple skyrmion phases: We have investigated how XXZ-type anisotropic interlayer exchange interactions stabilize various skyrmion crystal phases in a bilayer triangular-lattice spin model with staggered Dzyaloshinskii – Moriya interaction [4]. Through simulated annealing, we have revealed a rich magnetic phase diagram featuring multiple skyrmion crystal phases, including fractional and distorted types, depending on the interlayer anisotropy and external magnetic field. The results highlight how interlayer spin coupling modifies the relative positions of skyrmion cores across layers and facilitates topological spin textures in centrosymmetric systems.

(v) Stabilization mechanisms of magnetic skyrmion crystal and multiple-Q states based on momentum-resolved spin interactions: We have reviewed the theoretical framework for stabilizing magnetic skyrmion crystals and other multiple-Q spin textures using a momentum-resolved effective spin model [5]. We have shown taht the momentum-resolved effective spin model systematically classifies various stabilization mechanisms, such as Dzyaloshinskii – Moriya interaction, biquadratic interaction, anisotropy, and multi-sublattice effects, across both centrosymmetric and noncentrosymmetric crystals. The model captures diverse topological spin states, including hedgehog, meron-antimeron, and bubble crystals, offering a unified approach to explain experimental phase diagrams and predict novel magnetic phases in quantum materials.

References

[1] S. Hayami, Phys. Rev. B **109**, 184419 (2024).

[2] S. Hayami, Phys. Rev. B **110**, 014404 (2024).

[3] S. Hayami, J. Magn. Magn. Mater. **604**, 172293 (2024).

[4] S. Hayami, J. Magn. Magn. Mater. **619**, 172876 (2024).

[5] S. Hayami and R. Yambe, Mater. Today Quantum **3**, 100010 (2024).

Analyzing Ferromagnetic Order in Multi-Component Fermionic Systems using DMFT

Akihisa Koga
Department of Physics, Institute of Science Tokyo
Meguro, Tokyo 152-8551

Low-temperature properties in correlated fermion systems have attracted much attention since the discovery of high-T_c cuprates. In strongly correlated electron systems, spin degrees of freedom play a crucial role in stabilizing intriguing low-temperature phenomena such as magnetism, superconductivity, and Mott transitions. Orbital degrees of freedom further enrich the emergent behavior in these systems. Recently, optical lattice systems—periodic potentials imposed on ultracold atoms—have emerged as promising platforms for simulating strongly correlated models. In such systems, various parameters such as hopping amplitudes, interaction strengths, and lattice geometries can be precisely controlled. Furthermore, spin and orbital degrees of freedom can be introduced, enabling the realization of multicomponent strongly correlated fermionic systems.

One fundamental question is how symmetry-breaking states emerge in such multicomponent systems. In our previous work [1], we have investigated the half-filled Hubbard model with repulsive interactions to explore the instability toward antiferromagnetic order. By contrast, ferromagnetic instability in SU(N) Hubbard models remains poorly understood, especially beyond the SU(2) case. In the strong-coupling limit of the SU(2) Hubbard model, the motion of a single hole on a closed-loop lattice leads to a fully spin-polarized ground state—a phenomenon known as Nagaoka ferromagnetism. Although similar behavior has been reported in the SU(3) case [2], it remains an open question whether such ferromagnetic order persists at finite doping. In this regime, it is essential to treat strong Coulomb interactions and the low-energy itinerant behavior of electrons on an equal footing.

In this project, we investigate multicomponent fermionic systems described by the SU(N) Hubbard model and examine how ferromagnetic order emerges at low temperatures. To take strong particle correlations into account, we employ dynamical mean-field theory (DMFT) combined with the continuous-time quantum Monte Carlo (CTQMC) method. This approach allows us to treat strong correlations non-perturbatively and access low-temperature regimes relevant to magnetic ordering. Preliminary calculations suggest that ferromagnetic order emerges upon hole doping around one-third filling. Further detailed simulations and analyses are ongoing and will be reported in a forthcoming publication [3].

References

[1] H. Yanatori and A. Koga, Phys. Rev. B 94, 041110 (2016).

[2] H. Katsura and A. Tanaka, Phys. Rev. A 87, 013617 (2013).

[3] J. Fujii, K. Yamamoto and A. Koga, to be submitted.

Theoretical design of candidates for multilayer nickelate superconductors

KAZUHIKO KUROKI
Department of Physics, Osaka University
1-1 Machikaneyama, Toyonaka, Osaka, 560-0043, Japan

Theoretical studies have shown that the superconducting T_c in the bilayer Hubbard model can be higher than that of the d-wave superconducting state in the single-orbital Hubbard model [1, 2]. Hence, a realization of the bilayer Hubbard model in actual materials is a promising path toward finding new high temperature superconductors. Along this path, we previously proposed that a double layer Ruddlesden-Popper compound $La_3Ni_2O_7$ can be a good candidate for realizing the bilayer Hubbard model that satisfies the abovementioned conditions [3].

Recently, this material $La_3Ni_2O_7$ was found to exhibit high T_c superconductivity with a highest T_c of about 80 K under pressure above 14 GPa [4]. Inspired by this experiment, we theoretically revisited the possibility of superconductivity in $La_3Ni_2O_7$ by constructing a four-orbital model that takes into account the crystal structure at high pressures, and applying fluctuation exchange approximation to the model. We find that $s\pm$-pairing superconductivity, which is somewhat similar to that of the bilayer Hubbard model, can take place with high T_c that is consistent with the experimental observation[5].

Moreover, we further studied the possibility of superconductivity in a trilayer Ruddlesden-Popper nickelate $La_4Ni_3O_{10}$ under pressure. Since experiments on $La_3Ni_2O_7$ suggest that superconductivity takes place when the crystal structure becomes tetragonal ($I4/mmm$ symmetry) under pressure, it is natural to assume that a similar condition should be necessary for superconductivity to take place in $La_4Ni_3O_{10}$. Through DFT calculations, we found that a structural phase transition from monoclinic to tetragonal takes place around 15 GPa. Using the tetragonal crystal structure, we have theoretically investigated the possibility of superconductivity, where a combination of fluctuation exchange approximation and linearized Eliashberg equation is applied to a six-orbital model constructed from first principles band calculation. The obtained results suggests that $La_4Ni_3O_{10}$ may also become superconducting under high pressure with T_c comparable to relatively low T_c cuprates, although it is not as high as $La_3Ni_2O_7$[6]. This theoretical expectation was confirmed from experiments on polycrystalline samples[6].

There is now growing desire to realize bulk high T_c superconductivity at ambient pressure. In R6 fiscal year, we have theoretically designed a new material, $Sr_3Ni_2O_5Cl_2$, for which we predicted that the crystal structure takes $I4/mmm$ symmetry at ambient pressure[7]. Here, we have replaced La by Sr to raise the tolerance factor, and replaced the two outer apical O by Cl to partially compensate the number of electrons in Ni (Fig.1(a)(b)). Our phonon calculation performed for the structure with $I4/mmm$ symmetry at ambient pressure exhibit no imaginary modes (Fig.1(c)), showing that this structure is dynamically stable. Our fluctuation exchange study on this material shows that the T_c can be comparable to pressurized $La_3Ni_2O_7$[7]. Although this material had never been synthesized in the past, quite recently, Takano's group at NIMS succeeded in high pressure synthesis of this material[8], and found that the crystal structure indeed takes $I4/mmm$ symmetry at ambient pressure. Although superconductivity has not been observed at present, certainly more experiments are necessary to understand the nature of this new material.

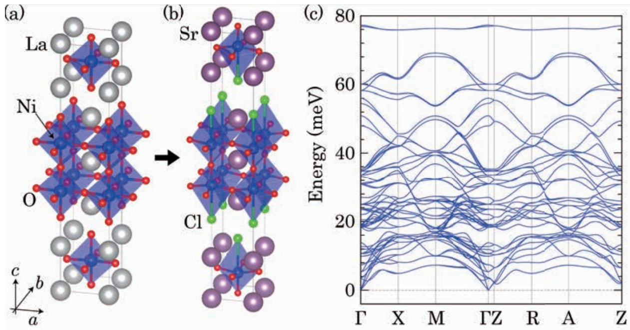

FIG. 1. (a) Crystal structure of $La_3Ni_2O_7$ at high pressure. (b) Crystal structure and (c) phonon band dispersion for $Sr_3Ni_2O_5Cl_2$ without applying pressure. Panels (b) and (c) are shown for the space group of $I4/mmm$. Crystal structures in this paper were depicted using the VESTA software [9]. Phonon dispersions in this paper were depicted in the Brillouin zone of the conventional tetragonal lattice.

[1] K. Kuroki, T. Kimura, and R. Arita, Phys. Rev. B **66**, 184508 (2002).
[2] V. Mishra, D. J. Scalapino, and T. A. Maier, Sci.

Rep. **6**, 32078 (2016).
[3] M. Nakata, D. Ogura, H. Usui, and K. Kuroki, Phys. Rev. B **95**, 214509 (2017).
[4] H. Sun, M. Huo, X. Hu, J. Li, Z. Liu, Y. Han, L. Tang, Z. Mao, P. Yang, B. Wang, J. Cheng, D.-X. Yao, G.-M. Zhang, and M. Wang, Nature (2023).
[5] H. Sakakibara, N. Kitamine, M. Ochi, and K. Kuroki, Phys. Rev. Lett. **132**, 106002 (2024).
[6] H. Sakakibara, M. Ochi, H. Nagata, Y. Ueki, H. Sakurai, R. Matsumoto, K. Terashima, K. Hirose, H. Ohta, M. Kato, Y. Takano, and K. Kuroki, Phys. Rev. B **109**, 144511 (2024).
[7] M. Ochi, H. Sakakibara, H. Usui, and K. Kuroki, Phys. Rev. B **111**, 064511 (2025).
[8] K. Yamane, Y. Matsushita, S. Adachi, R. Matsumoto, K. Terashima, T. Hiroto, H. Sakurai, and Y. Takano, Acta Cryst. **C81**, 259 (2025).
[9] K. Momma and F. Izumi, J. Appl. Crystallogr. **44**, 1272 (2011).

Field-driven spin structure and magnetization plateau in a spinel ferrimagnet $MnCr_2S_4$

Hidemaro SUWA
Department of Physics, University of Tokyo, Tokyo 113-0033

Many interesting magnetic materials behave in unexpected ways because the local spins inside them cannot all point in directions that keep every neighbour happy. This situation is called magnetic frustration, and it can lead to exotic states of matter such as spin liquids, multiferroics, or supersolid-like magnets. Spinel crystals whose chemical formula is AB_2X_4 are a playground for such behaviour because their crystal lattice forces the spins on the A and B sites into two different, competing arrangements.

We studied the sulphur spinel $MnCr_2S_4$, in which the A site hosts manganese ions (Mn^{2+}) and the B site hosts chromium ions (Cr^{3+}). At ordinary temperatures the spins point every which way (a paramagnet). On cooling to about 65 K they lock into a ferrimagnetic pattern: the manganese and chromium sublattices point in opposite directions, so the whole crystal keeps a net magnetisation. Cooling further, below ≈ 5 K, the spins tilt away from perfect opposition and form a special canted arrangement known as a Yafet–Kittel (YK) phase.

Things become even richer when we apply very strong magnetic fields. At low temperatures we observed a sequence of five field-driven transitions at roughly 11 T, 25 T, 50 T, 75 T and 85 T. Between 25 T and 50 T the magnetisation plateaus at exactly 6 μB per formula unit—a hallmark of strong coupling between the spins and the crystal lattice (spin-lattice coupling). Theoretical work suggests some of these field-induced phases behave like spin superfluids or supersolids.

Previous neutron studies of $MnCr_2S_4$ were carried out on powdered samples and only in zero field, leaving several open questions: Is the low-temperature YK phase real or an artefact? What exact spin patterns appear in the various high-field phases? How does the interaction between manganese and chromium spins evolve with field?

To answer these questions, we performed a large-scale Monte Carlo simulation of a frustrated spin-lattice model on ISSP System B in the class C project (2024-Ca-0073) in an MPI parallel computation using up to eight nodes simultaneously. We nailed down the spin structre for each phase by comparing our simulation to a neutron-diffraction experiment combining conventional powder measurements and high-resolution single-crystal experiments in magnetic fields up to 35 T. By analysing the data together with mean-field calculations, we determined how the manganese–manganese and manganese–chromium exchange couplings change from one phase to the next and how strongly the lattice participates in those changes. Our results clarified the complete magnetic phase diagram of $MnCr_2S_4$ and provide a solid starting point for future theories of frustrated spin-lattice systems.

References

[1] F. Duc, N. Qureshi, H. Suwa, et al., Phys. Rev. B. **110**, 214416 (2024).

Spin Nematics and Spin Liquids in S=1 magnets

Rico Pohle

Creative Science Unit,

Faculty of Science, Shizuoka University, Shizuoka 422-8529

We have studied the thermodynamic and dynamical properties of unconventional magnets composed of atoms with higher spin S. In particular, we focused on magnets made of S=1 moments due to their connection with spin nematic phases – magnetically ordered states where the order arises not from spin-dipole moments, but from spin-quadrupole moments. To investigate these systems, we have utilized a novel method based on a $U(3)$ formalism [1]. This method enables us to compute finite-temperature properties via Monte Carlo simulations (u3MC) and dynamical properties via molecular dynamics simulations (u3MD) for S=1 magnets on any type of lattice. Our codes have been efficiently implemented with large-scale CPU parallelization on the ISSP supercomputer. During the fiscal year FY2024, we achieved significant progress on the following topics:

(i) Simulation of gravitational waves from spin nematic phases: Fluctuations away from ferroquadrupolar order in spin nematics can be described by higher-rank tensor fields. In this project, we compared the action governing quadrupolar fluctuations in spin nematics to the action of spacetime fluctuations in flat space, and found that their mathematical structures are closely related. This opens a new avenue for studying gravitational wave physics within a microscopic condensed matter system. We supported this theoretical proposal with numerical simulations of vortex-pair annihilation processes in a spin nematic state, suggesting a potential direction for experimental observation in cold atom systems [2].

(ii) Interplay of spin nematics and spin liquids in S=1 Kitaev models: We investigated the interplay between spin nematic phases and spin liquids in the S=1 Kitaev model with bilinear-biquadratic (BBQ) interactions using the u3MC and u3MD simulation methods. We discovered that the model stabilizes a chiral spin liquid, which we analyzed further by simplifying the model to a discretized eight-color model [3]. We found that the chiral spin liquid can be interpreted as an example of classical topological order, after mapping it to a Z_2 lattice gauge theory. We confirmed our physical understanding and interpretations through classical Monte Carlo simulations [4].

(iii) S=1 BBQ model on the pyrochlore lattice and application to $NaCaNi_2F_7$: We studied the phase diagram of the S=1 BBQ model on the pyrochlore lattice using u3MC and u3MD simulations. We identified up to seven distinct spin liquid phases and proposed that $NaCaNi_2F_7$ is proximate to a nematic spin liquid, where strong biquadratic interactions drive a finite-temperature transition that breaks spin rotational symmetry while retaining a residual $U(1)$ degree of freedom. We also showed that dynamics of quadrupolar moments reveal a gapless Goldstone mode and proposed a mechanism for the observed spin glass transition based on weak anisotropic spin interactions perturbing the nematic spin liquid state [5].

References

[1] K. Remund *et al.*, Phys. Rev. Research **4**, 033106 (2022).

[2] L. Chojnacki *et al.*, Phys. Rev. B **109**, L220407 (2024) [Editor's suggestion].

[3] R. Pohle, N. Shannon, and Y. Motome, Phys. Rev. Research **6**, 033077 (2024).

[4] H. Yan and R. Pohle, Phys. Rev. Research **7**, L012052 (2025).

[5] R. Pohle and N. Shannon, preprint (arXiv:2503.12776).

Novel Quantum Phases with Current and Spin Current Textures due to Electron Correlation

Takami TOHYAMA
Department of Applied Physics, Tokyo University of Science, Katsushika, Tokyo 125-8585

Unexpected phenomena often emerge in quantum many-body systems, and they are most pronounced when strong quantum fluctuations are present in strongly correlated electron systems. Such phenomena have recently observed in kagome metals $A\mathrm{V}_3\mathrm{Sb}_5$ (A=Cs, Rb, K). In these compounds, unconventional superconductivity, time-reversal symmetry breaking, and nematic order have been reported in the presence of charge orders. Based on a single-orbital Hubbard model on a kagome lattice, an inverse star of David-type bond order as well as a charge-loop current order has been proposed theoretically [1]. However, there are few studies that investigate the ground state of the model by unbiased numerical calculations.

In this project, we investigate the ground state properties of the single-orbital kagome Hubbard model using the density-matrix renormalization group (DMRG) method whose computational code has been developed by our group. We use a 76-site rhombus lattice with six triangles along one direction (open boundary condition) and four triangles along the other direction (periodic boundary condition) and the ratio of on-site Coulomb interaction U and nearest-neighbor hopping t to be $U/t = 6$ and 10. The bond dimension of the DMRG procedures is maximally set to be 10,000 and a snake-type geometry is taken for one-dimensional sweeping in DMRG.

The electron-density and bond-density distributions are calculated for $n = 0.95$, 0.84, and 0.74, whose numbers are determined by the fact that the Fermi level of $A\mathrm{V}_3\mathrm{Sb}_5$ is close to a van Hove singularity (vHS) point in a non-interacting kagome band structure. We find that the inverse star of David-type bond order is formed only at $n = 0.84$ (close to the vHS point) for both $U/t = 6$ and 10 [3]. At the same time, a charge order is seen in the density profile at $n = 0.84$. We also calculate the spatial distribution of charge and spin currents around a bond to which a pinning field is applied. This method has been applied to several types of Hubbard models and spin loop-current textures have been proposed for a charge-modulated system such as a stripe phase of the Hubbard model on a square lattice [2]. We find that only the $n = 0.84$ case induces charge and spin currents near the bond with a pinning field. These findings indicate that vHS in a kagome lattice under the presence of strong correlation plays a crucial role in generating unexpected quantum phenomena.

References

[1] R. Tazai, Y. Yamakawa, and H. Kontani: Nat. Commun. **14**, 7845 (2023).

[2] K. Shinjo, S. Sota, S. Yunoki, and T. Tohyama: Phys. Rev. B **108**, 195118 (2023).

[3] T. Tohyama *et al.*, in preparation.

Research of Quantum Critical Points in the Vicinity of Three-Channel Kondo Phase

Takashi HOTTA
Department of Physics, Tokyo Metropolitan University
1-1 Minami-Osawa, Hachioji, Tokyo 192-0397

For the purpose to promote our understanding on the emergence of three-channel Kondo effect from Ho ions for the case with Γ_5 triplet ground state [1], we have attempted to investigate quantum critical points around the three-channel Kondo state in the phase diagram on the V_8-V_7 plane, where V_7 and V_8 denote the hybridization of localized Γ_7 and Γ_8 electrons with the conduction bands, respectively.

Let us start our discussion on the exhibition of the model Hamiltonian. First we define one f-electron state by the eigenstate of spin-orbit and crystalline electric field (CEF) potential terms. Under the cubic CEF potential, we obtain Γ_7 doublet and Γ_8 quartet from $j = 5/2$ sextet, whereas we find Γ_6 doublet, Γ_7 doublet, and Γ_8 quartet from $j = 7/2$ octet. Next we include the Γ_7 and Γ_8 conduction electron bands. Note that we consider only the hybridization between the conduction and $j = 7/2$ electrons to consider heavy rare-earth ion such as Ho^{3+}. Then, we obtain the model Hamiltonian as

$$\begin{aligned} H &= \sum_{\boldsymbol{k},\mu,\tau} \varepsilon_{\boldsymbol{k}} c^{\dagger}_{\boldsymbol{k}\mu\tau} c_{\boldsymbol{k}\mu\tau} + \sum_{\boldsymbol{k},\mu,\tau} V_{\mu} (c^{\dagger}_{\boldsymbol{k}\mu\tau} f_{b\mu\tau} + \text{h.c.}) \\ &+ nE_f + \sum_{j,\mu,\tau} (\lambda_j + B_{j,\mu}) f^{\dagger}_{j\mu\tau} f_{j\mu\tau} \\ &+ \sum_{j_1\sim j_4} \sum_{\mu_1\sim\mu_4} \sum_{\tau_1\sim\tau_4} I^{j_1 j_2, j_3 j_4}_{\mu_1\tau_1\mu_2\tau_2,\mu_3\tau_3\mu_4\tau_4} \\ &\times f^{\dagger}_{j_1\mu_1\tau_1} f^{\dagger}_{j_2\mu_2\tau_2} f_{j_3\mu_3\tau_3} f_{j_4\mu_4\tau_4}, \end{aligned} \tag{1}$$

where $\varepsilon_{\boldsymbol{k}}$ denotes the dispersion of conduction electron with wave vector $\boldsymbol{k}$, $c_{\boldsymbol{k}\mu\tau}$ indicates the annihilation operator of a conduction electron, $f_{j\mu\tau}$ is the annihilation operator of a localized f electron in the bases of (j, μ, τ), j denotes the total angular momentum, $j = 5/2$ and $7/2$ are denoted by "a" and "b", respectively, μ distinguishes the cubic irreducible representation, Γ_8 states are distinguished by $\mu = \alpha$ and β, while the Γ_7 and Γ_6 states are labeled by $\mu = \gamma$ and δ, respectively, τ denotes the pseudo-spin, which distinguishes the degeneracy concerning the time-reversal symmetry, V_μ denotes the hybridization between f electron in the μ orbital and conduction electron of the μ band, n is the local f-electron number at an impurity site, and E_f is the f-electron level to control n.

As for the spin-orbit term, we obtain $\lambda_a = -2\lambda$ and $\lambda_b = (3/2)\lambda$, where λ is the spin-orbit coupling of f electron. Here we set $\lambda = 0.265$ eV for Ho ion. Concerning the CEF potential term for $j = 5/2$, we obtain $B_{a,\alpha} = B_{a,\beta} = 1320B_4^0/7$ and $B_{a,\gamma} = -2640B_4^0/7$, where B_4^0 denotes the fourth-order CEF parameter for the angular momentum $\ell = 3$. For $j = 7/2$, we obtain $B_{b,\alpha} = B_{b,\beta} = 360B_4^0/7 + 2880B_6^0$, $B_{b,\gamma} = -3240B_4^0/7 - 2160B_6^0$, and $B_{b,\delta} = 360B_4^0 - 3600B_6^0/7$. In the following calculations, we use the parametrization as $B_4^0 = Wx/15$ and $B_6^0 = W(1 - |x|)/180$ for $\ell = 3$, where x specifies the CEF scheme for the O_{h} point group, while W determines the energy scale of the CEF potentials. In this work, we set $W = 10^{-3}$ eV and treat x as the parameter to control the CEF ground state.

For the Coulomb interaction terms, we do not show the explicit forms of I here, but they are expressed by the four Slater-Condon parameters, F^0, F^2, F^4, and F^6. These values should be determined from experimental results, but here we simply set the ratio as $F^0/10 = F^2/5 = F^4/3 = F^6 = U$, where U indicates the Hund's rule interaction among the f orbitals. In this work, we set $U = 1$ eV.

Concerning the electron hybridization, we introduce $V_7 = V_\gamma$ and $V_8 = V_\alpha = V_\beta$ with $V_\delta = 0$. In the previous research, we have considered only the case of $V_7 = V_8$ [1], but in the present research, we treat the general case of $V_7 \neq V_8$ to depict the ground-state phase diagram including the three-channel Kondo state.

We have analyzed the three-band Anderson model by exploiting a numerical renormalization group (NRG) method. We introduce a cut-off Λ for the logarithmic discretization of the conduction band. Due to the limitation of computer resources, we keep M low-energy states. Here we use $\Lambda = 8$ and $M = 5,000$. In the NRG calculation, the temperature T is defined as $T = D\Lambda^{-(N-1)/2}$, where D is half the conduction band width, which is set as 1 eV, and N is the number of renormalization steps.

We briefly explain our previous result [1]. From the NRG calculations for the case of $V_7 = V_8$, we have unveiled the three-channel Kondo effect for the local Γ_5 triplet ground state, characterized by a residual entropy $S_{\rm imp}(0)$ of $\log\phi$ with the golden ratio $\phi = (1+\sqrt{5})/2$.

In order to seek for the relation between the quantum criticality and the emergence of the three-channel Kondo phase, we have attempted to depict the ground-state phase diagram on the V_8-V_7 plane, by repeating the NRG calculations for a thousand of parameter sets (V_8, V_7). To understand the ground-state property, we have checked the temperature dependence of entropy $S_{\rm imp}(T)$ and the change of the energy spectra as functions of NRG steps. The details will be discussed elsewhere [2], but here we show a part of the results.

In Fig. 1, we show the ground-state phase diagram on the V_8-V_7 plane in the region of $0 < V_8 \leq 1.2$ and $0 < V_7 \leq 1$. We note a quantum critical point (QCP) on the line of $V_7 = 0$ around $V_8 \approx 0.8$, characterized by the residual entropy $S_{\rm imp}(0) = \log\sqrt{2}$. This QCP is well known to appear between the Kondo singlet and the CEF singlet phases. Note that in the present case, the Kondo singlet appears for small V_8 from the screening of local Γ_5 triplet.

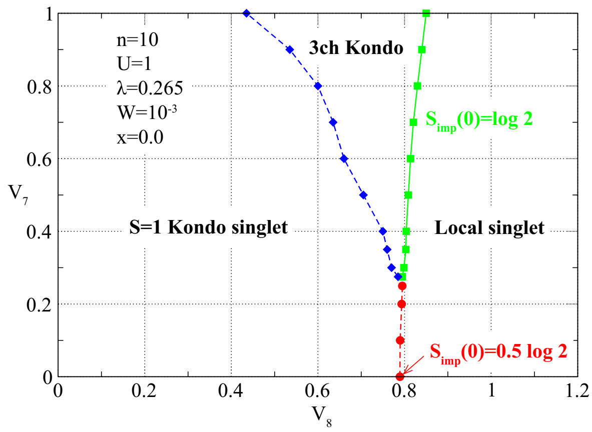

Figure 1: Ground-state phase diagram on the V_8-V_7 plane in the region of $0 < V_8 \leq 1.2$ and $0 < V_7 \leq 1$.

With the increase of the value of V_7 near the QCP, the residual entropy of $\log\sqrt{2}$ is found to disappear, while the sudden change in the energy spectrum still remains, corresponding to the change in the ground state from the Kondo singlet to the local singlet phase. When we further increase V_7 up to 0.3, we encounter the three-channel Kondo phase between the Kondo singlet and the local singlet phases. Note that the boundary between the three-channel Kondo and the local singlet phases is characterized by a residual entropy of $\log 2$ [1]. We have noticed that the three-channel Kondo phase eventually disappears when we further increase V_7, but the final destination will be discussed in the near future [2].

References

[1] T. Hotta, J. Phys. Soc. Jpn. **90**, 113701 (2021).

[2] T. Hotta, in preparation.

Spin fluctuations and superconductivity in f-electron compounds under pressure

Makoto SHIMIZU
Department of Physics, Graduate School of Science, Kyoto University
Kyoto 606-8502, Japan

A heavy-fermion paramagnet UTe_2 has been a strong candidate for a spin-triplet superconductor. Experiments on UTe_2 under pressure have been vigorously conducted, and rich phase diagrams have been suggested. We study the electronic structure of the compound under pressure based on the density functional theory (DFT) with employing structural optimization. For structural optimization, we use VASP installed on the ISSP supercomputers.

As a result, the low-energy band structure and Fermi surfaces are not sensitive to pressure for parameters where itinerant f-electrons are not essential. However, we find a significant pressure dependence for a certain Coulomb interaction U of the GGA+U calculation, where the large weight of f-electrons appears at the Fermi level. An increase in the density of states at the Fermi level is observed under pressure, which is attributed to compressive stress along the [010] crystallographic axis.

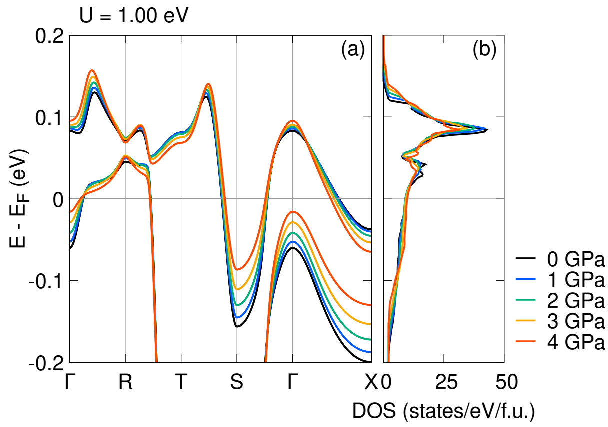

Figure 1: (a) Band structure and (b) density of states of UTe_2 under hydrostatic pressure within GGA+U where $U = 1$ eV.

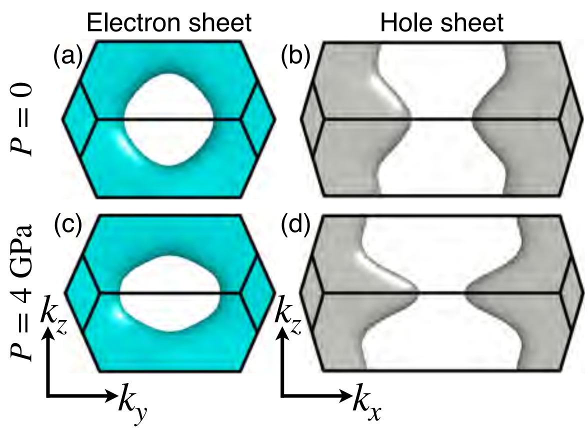

Figure 2: Fermi surface of UTe_2 under hydrostatic pressure within GGA+U where $U = 1$ eV.

References

[1] M. Shimizu, and Y. Yanase, arXiv:2408.04292.

Nonequilibrium phenomena in strongly correlated systems

Robert Peters

Department of Physics

Graduate School of Science, Kyoto University, Kyoto 606-8502

Understanding emergent phenomena in strongly correlated and topologically nontrivial materials requires high-precision numerical simulations that go beyond analytical treatments. Leveraging large-scale computational resources, we investigated (i) nonlinear response functions in magnetic materials and (ii) quantum dynamics in spin systems using neural network quantum states.

Nonlinear Responses in Correlated and Topological Magnetic Systems

In recent years, nonlinear spintronics has emerged as a promising frontier for the control and detection of spin phenomena that goes beyond linear response theory. Using supercomputing resources, we numerically evaluated second-order response functions in strongly correlated systems and magnets, focusing on two key phenomena: the nonlinear Edelstein effect (NEE) and the nonlinear magnetoelectric effect (NMEE).

In the first study [1], we investigated the NEE in a correlated electron system described by a Hubbard model. Our simulations revealed that electron correlations can significantly modify the magnitude of the nonlinear spin response. Specifically, the real part of the electronic self-energy enhances the NEE, while the imaginary part leads to suppression. The NEE was also found to be closely related to optically induced spin currents and the inverse Faraday effect, providing a bridge to nonlinear optical spintronics.

In the second study [2], we explored the NMEE in systems with magnetic octupole order, such as a d-wave altermagnet and a pyrochlore lattice with all-in/all-out magnetic order. We calculated the NMEE tensor using quantum kinetic theory and confirmed its significant magnitude through detailed numerical simulations. Notably, in the magnetic Weyl semimetal phase of the pyrochlore lattice, the NMEE is strongly enhanced near Weyl nodes due to the contribution of the quantum metric in the response tensor. These results provide a pathway for detecting hidden multipolar orders through nonlinear magneto-optical measurements.

Quantum Dynamics with Neural Network Quantum States

In a separate project, we investigated the real-time dynamics of quantum skyrmions using neural network quantum states (NNQS) [3]. Employing variational Monte Carlo with a restricted Boltzmann machine as the wavefunction ansatz, we first obtained the ground state of a quantum Heisenberg model with Dzyaloshinskii-Moriya interaction. Using the time-dependent variational principle, we simulated the evolution of quantum skyrmions under a magnetic field gradient.

Our results show that field gradients are a powerful tool for controlling skyrmion motion in quantum spin systems. Furthermore, we observed skyrmion decay due to interactions, highlighting the importance of quantum effects in skyrmion dynamics. These calculations demonstrate that NNQS can access quantum real-time dynamics in regimes inaccessible to conventional exact diagonalization.

References

[1] Jun Ōiké and Robert Peters, *Phys. Rev. B* **110**, 165111 (2024).

[2] Jun Ōiké, Koki Shinada, and Robert Peters, *Phys. Rev. B* **110**, 184407 (2024).

[3] Ashish Joshi, Robert Peters, and Thore Posske, *Phys. Rev. B* **110**, 104411 (2024).

Computational Studies of Pressure Effects on Electronic Correlations and Superconductivity in Organic Conductors

Kazuyoshi Yoshimi
Institute for Solid State Physics, University of Tokyo
Kashiwa-no-ha, Kashiwa, Chiba 277-8581

The objective of this research is to estimate detailed crystal structures under pressure and predict functional properties of strongly correlated materials using *ab–initio* calculations. Special attention is given to organic molecular solids, where pressure significantly affects electronic properties, including charge/spin ordering, superconductivity, and topological phenomena. Based on crystal structure data obtained from experimental groups, we derived low-energy effective models under pressure and quantitatively analyzed electronic correlation effects. We also performed first-principles calculations to optimize structures obtained under ambient pressure and verified consistency with experimental results. As a large number of systematic calculations were required for various pressure conditions, scripts were generated for bulk jobs using Moller [4] and exhaustive calculations were carried out for several pressure conditions in order to significantly improve the efficiency of the calculations.

In this study [5], single-crystal X-ray diffraction experiments on the organic conductor $(TMTTF)_2PF_6$ were performed under pressures up to 8 GPa, enabling precise structural determination. Using these structures, we conducted first-principles calculations with Quantum ESPRESSO [1] and derived low-energy effective models using RESPACK [2], based on the calculated band structures and Wannier functions. These models were then analyzed using mVMC [3], thoroughly evaluating the stability of charge and spin ordering under pressure.

As a result of the significant decrease in crystal volume with increasing pressure, the conduction bandwidth is broadened and the screen-Coulomb interaction is dramatically reduced. Additionally, the degree of dimerization in the conduction bands sharply decreased and nearly vanished above 3 GPa, significantly diminishing the strength of electronic correlations. Furthermore, we confirmed a good agreement between experimental resistivity measurements and theoretical analysis. Specifically, the stability of spin-density wave (SDW) and charge ordering (CO), derived from theoretical calculations, was consistent with experimental resistivity data. The CO notably became unstable above approximately 1 GPa, while the SDW persisted at higher pressures. These outcomes clarify the differences between physical and chemical pressures [6] and deepen the understanding of unified phase diagrams.

Additionally, we performed X-ray structural analysis and electronic structure calculations under pressure on the organic superconductor β'-$(ET)_2ICl_2$ [7]. Our findings revealed a Lifshitz transition around 6 GPa, changing the Fermi surface from one-dimensional to two-dimensional. Concurrently, the on-site Coulomb interaction significantly decreased, reaching approximately half its ambient-pressure value around 10 GPa.

These results provide crucial insights into the mechanism of superconductivity under high pressure and elucidate the significant impact of pressure-induced electronic structure changes on superconductivity in organic materials.

References

[1] P. Giannozzi, O. Andreussi, T. Brumme *et al.*, J. Phys. Condens. Matter. **29**, 465901(2017).

[2] K. Nakamura, Y. Yoshimoto, Y. Nomura *et al.*, Comput. Phys. Commun., **261**, 107781 (2021).

[3] T. Misawa, S. Morita, K. Yoshimi *et al.*, Comput. Phys. Commun. **235**, 447 (2019).

[4] https://github.com/issp-center-dev/Moller.

[5] M. Itoi, K. Yoshimi, H. Ma *et al.*, Phys. Rev. Research **6**, 043308.

[6] K. Yoshimi, T. Misawa, T. Tsumuraya, and H. Seo, Phys. Rev. Lett. **131**, 036401 (2023).

[7] T. Kobayashi, K. Yoshimi, H. Ma *et al.*, Phys. Rev. Materials **9**, L021801 (2025).

Studies of the superconductivity and magnetic states in the strongly correlated electron systems using Hubbard models.

Atsushi Yamada
Department of Physics, Chiba University
Chiba 263-8522, Japana, Chiba 277-8581

Strong electron correlations lead to interesting phenomena such as superconductivity with various pairing symmetries and purely paramagnetic insulator (spin liquid) in low dimensional materials. The organic charge-transfer salts κ-(BEDT-TTF)$_2$Cu$_2$(CN)$_3$ [1, 2, 3, 4, 5, 6, 7] is a good example of such materials, whose spin liquid state transits to a superconductor with d_{xy} pairing symmetry at $T_K = 3.9$ K upon applying pressure [5, 6].

The superconductivity(SC) of this material was studied theoretically using the Hubbard model on the isotropic triangular lattice, which is a simple effective Hamiltonian of this material[8] described by the hopping t and the on-site Coulomb repulsion U.

We have studied d-wave superconductivity(SC) in this model at zero temperature and half-filling using the variational cluster approximation[9]. We found that the d_{xy} SC is the ground state below the Mott insulator phase $U/t \lesssim 6$, and the energy of chiral $d + id$ SC is slightly higher than the d_{xy} SC. The energy difference between the normal and d_{xy} states is about $0.02t \sim 0.06t$ for $U/t \simeq 4 \sim 5$. This result is semi-quantitatively consistent with the SC transition temperature $T_K = 3.9$ K of κ-(BEDT-TTF)$_2$Cu$_2$(CN)$_3$, where t is estimated to be about 0.06 eV, and the predicted pairing symmetry d_{xy} agrees with the STM observations. The energy difference between the $d + id$ and d_{xy} is about $0.01t \sim 0.03t$ for $U/t \simeq 4 \sim 5$ so the transition from $d + id$ to d_{xy}, or some effects of $d + id$ in d_{xy} phase may be observed in experiments for κ-(BEDT-TTF)$_2$Cu$_2$(CN)$_3$.

References

[1] S. Lefebvre, P. Wzietek, S. Brown, C. Bourbonnais, D. Jérome, C. Mézière, M. Fourmigué, and P. Batail, Phys. Rev. Lett. **85**, 5420 (2000).

[2] Y. Shimizu, K. Miyagawa, K. Kanoda, M. Maesato, and G. Saito, *et al.*, Phys. Rev. Lett. **91**, 107001 (2003).

[3] F. Kagawa, T. Itou, K. Miyagawa, and K. Kanoda, Phys. Rev. B **69**, 064511 (2004).

[4] Y. Kurosaki, Y. Shimizu, K. Miyagawa, K. Kanoda, and G. Saito, Phys. Rev. Lett. **95**, 177001 (2005).

[5] K. Izawa, H. Yamaguchi, T. Sasaki and Y. Matsuda, Phys. Rev. Lett. **88** 027002 (2001).

[6] K. Ichimura and K. Nomura, J. Phys. Soc. Jpn. **75**, 051012 (2006).

[7] R.S. Manna, M. de Souza, A. Brühl, J.A. Schlueter, and M. Lang, Phys. Rev. Lett. **104**, 016403 (2010).

[8] H. Kino and H. Fukuyama, J. Phys. Soc. Jpn. **65**, 2158 (1996).

[9] A. Yamada, J. Phys. Soc. Jpn. **94**, 044705 (2025).

Electron correlation in strongly interacting electron systems

Takashi YANAGISAWA
National Institute of Advanced Industrial Science and Technology (AIST)
1-1-1 Umezono, Tsukuba, Ibaraki 305-8568, Japan

1 Introduction

In our numerical research, we use the optimized many-body wave functions to study electronic properties of strongly correlated electron systems. The expectation values are evaluated by using the Metropolis Monte Carlo procedure. We carried out parallel computations in Monte Carlo calculations. In order to reduce statistical errors, we performed ~ 500 parallel calculations. Parallel computing is very essential to reduce Monte Carlo statistical errors. The parallelization rate reached 99%.

We use the optimized many-body wave function which is improved by multiplying by off-diagonal exponential operators given by $e^{-\lambda K}$ and P_G where K is the kinetic energy part (non-interacting part) of the Hamiltonian and $P_G = P_G(g)$ is the Gutzwiller operator to control the double occupancy with the variational parameter g[1]. P_G is also written in the form $e^{-\alpha D}$. $\psi^{(1)} \equiv \psi_G = P_G\psi_0$ is the well known Gutzwiller wave function. We consider the many-body wave function given by $\psi^{(2)} \equiv \exp(-\lambda K)P_G\psi_0$, where ψ_0 indicates an initial wave function which is usually taken as the Fermi sea, the BCS wave function or the state with some magnetic (or charge) orders. We can improve the wave function systematically by multiplying by operators P_G and $e^{-\lambda K}$ further.

We can also consider $\psi^{(3)} \equiv P_G(g')\psi^{(2)}$ and $\psi^{(4)} \equiv \exp(-\lambda' K)P_G(g')\psi^{(2)}$ for different variational parameters λ' and g'. The wave function $\psi^{(4)}$ is a very good many-body wave function because the ground-state energy is lowered greatly and the ground-state energy is lower than those that are evaluated by using any other wave functions. We can further proceed to employ $\psi^{(5)}$ and $\psi^{(6)}$. We can also use the Jastrow-type wave function which is written as $\psi_J = P_G P_Q P_J \psi_0$ where P_J indicates a nearest-neighbor number correlation operator and P_Q controls the nearest-neighbor doublon-holon correlation.

2 Strong correlation effect on superconductivity

We have carried out variational Monte Carlo simulations to examine the ground state of the two-dimensional Hubbard model on a square lattice. We here examine the effect of strong correlation on superconductivity. The BCS wave function $\psi_{BCS}(\Delta_s)$ with the gap function Δ_s clearly shows the long-range correlation. In Fig. 1, we show the superconducting correlation function $D_{sc}(\ell) = \langle \Delta^\dagger(i)\Delta(i+\ell)\rangle$ as a function of lattice sites for $N_e = 88$, $U = 18t$ and $t' = 0$ on a 10×10 lattice[5]. Here the pair annihilation operator $\Delta(i)$ at the site i is given by

$$\Delta(i) = \Delta_x(i)+\Delta_{-x}(i)-(\Delta_y(i)+\Delta_{-y}(i)), \quad (1)$$

where $\Delta_\alpha = c_{i\downarrow}c_{i+\hat{\alpha}\uparrow} - c_{i\uparrow}c_{i+\hat{\alpha}\downarrow}$ for $\alpha = x$ and y. $\hat{\alpha}$ indicates the unit vector in the α-th direction. The pair correlation function $D_{sc}(\ell)$ shows that the long-range order of superconductivity indeed exists in the ground state. $D_{sc}(\ell)$ is, however, reduced by strong electron correlation since as shown in Fig. 1 the Gutzwiller projection operator suppresses the pair correlation considerably.

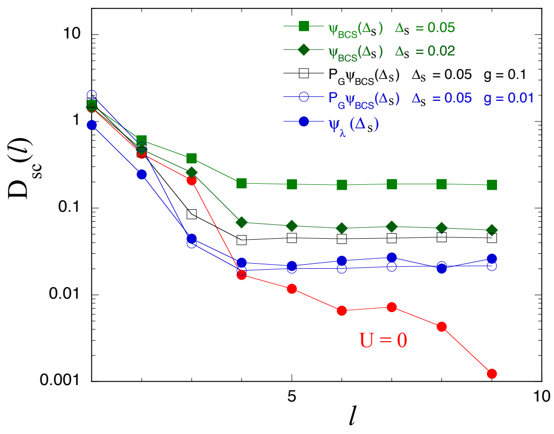

Figure 1: The pair correlation function $D_{sc}(\ell)$ as a function of the lattice site ℓ on a 10×10 lattice with $U = 18t$, $t' = 0$ and $N_e = 88$. The lattice sites ℓ are ℓ=(1,1), (1,2), (1,3), (1,4), (1,5), (2,5), (3,5), (4,5) and (5,5) and the site i is chosen as $i = (1, 1)$. The figure includes $D_{sc}(\ell)$ for $U = 0$, the non-interacting BCS wave function with the gap function $\Delta_s = 0.05$ and 0.02 and the the Gutzwiller projected BCS function with $\Delta_s = 0.05$. The result for ψ_λ indicates $D_{sc}(\ell)$ for the optimized wave function with $\Delta_s = 0.05$.

3 Charge-ordered state

We investigated the stability of charge-ordered state near the 1/8-doping region when $t' = 0$ and U/t is large. The one-particle state ψ_0 with inhomogeneous charge and spin orders are given by the eigenstate of the following Hamiltonian

$$H_{tri} = -\sum_{ij\sigma} t_{ij} c^\dagger_{i\sigma} c_{j\sigma} + \sum_{i\sigma} (\rho_i - \mathrm{sgn}(\sigma) m_i) n_{i\sigma}, \tag{2}$$

with $\rho_i = \rho\cos(\mathbf{Q}_c\cdot(\mathbf{r}_i - \mathbf{r}_0))$ and $m_i = m\sin(\mathbf{Q}_s\cdot(\mathbf{r}_i - \mathbf{r}_0))$. ρ and $m \equiv \Delta_{AF}$ are variational parameters. Here two incommensurate wave vectors $\mathbf{Q}_c$ and $\mathbf{Q}_s$ characterize the charge and spin configurations, respectively. We set $\mathbf{Q}_c = 2\mathbf{Q}_s$. $\mathbf{r}_0$ denotes the position of the domain boundary. The vertical stripe is represented by $\mathbf{Q}_s = (\pi \pm 2\pi\delta, \pi)$ where δ stands for the incommensurability.

We consider the case $t' = 0$. In this case, when U is as large as $U = 18t$, the antiferromagnetic state does not become stable[2] and thus a pure charge-ordered state can be stable in stead of stripes. This charge-ordered state can be called the nematic state. An important question is whether the charge-ordered state without magnetic order exists and then coexists with superconductivity. We indeed found that the charge-ordered state exists without magnetic ordering and this state coexists with superconductivity when the doping rate x is near 1/8 where we set $\delta = 1/8$[4, 5].

4 Summary

We examined the ground state of the two-dimensional Hubbard model by using the advanced optimized variational Monte Carlo method. We presented the d-wave pair correlation function as a function of lattice sites. We can show that the inhomogeneous charge-ordered state without magnetic ordering becomes stable for $t' = 0$ when the doping rate x is near $x = 0.125$. It is also shown that the d-wave superconductivity with a spatially oscillating gap function can coexist with charge ordering.

References

[1] T. Yanagisawa et al., J. Phys. Soc. Jpn. 67, 3867 (1998).
T. Yanagisawa, Phys. Rev. B75, 224503 (2007) (arXiv: 0707.1929).

[2] T. Yanagisawa, J. Phys. Soc. Jpn. 85, 114707 (2016).
T. Yanagisawa, J. Phys. Soc. Jpn. 88, 054702 (2019).
T. Yanagisawa, Condensed Matter 4, 57 (2019).

[3] T. Yanagisawa, Phys. Lett. A403, 127382 (2021).
T. Yanagisawa et al., EPL 134, 27004 (2021).

[4] M. Miyazaki, T. Yanagisawa, Phys. Lett. A448, 128276 (2022).

[5] T. Yanagisawa, High Temperature Materials 1, 10004 (2024).
T. Yanagisawa, preprint.

High harmonic generation in a spin scalar chiral state

Atsushi ONO
Department of Physics, Tohoku University
Sendai 980-8578

High harmonic generation (HHG) has emerged as a powerful tool for investigating ultrafast electron dynamics and reconstructing electronic band structures. Recent studies have demonstrated that HHG can also capture the geometric properties of electronic systems, such as the Berry curvature. However, while HHG in systems with broken spatial inversion symmetry has been extensively explored, studies of systems with broken time-reversal symmetry remain scarce.

In a paper [1], we numerically examined HHG in a spin scalar chiral state, where time-reversal symmetry is broken by the four-sublattice all-in/all-out spin structure, as depicted in Figs. 1(a) and 1(b). We considered the ferromagnetic Kondo lattice model on a triangular lattice, where electrons are driven within a fixed spin texture. Figure 1(c) presents the polarization angle dependence of the fifth harmonic intensity for scalar chiral states with positive (bold red curve) and negative (bold blue curve) chirality. We found that the sign of the scalar chirality significantly affects the harmonic intensity and that this effect predominantly appears in the component parallel to the polarization direction (thin orange and cyan curves), in contrast to the typically observed transverse responses of intraband currents. Our semiclassical analysis revealed that this behavior originates from interband currents induced by the recombination of electron–hole pairs whose real-space trajectories are modulated by the anomalous velocity.

These findings offer new insights into how topological spin textures and the Berry curvature imprint themselves on high harmonic spectra, highlighting the potential of HHG as a probe of geometry in magnetic materials.

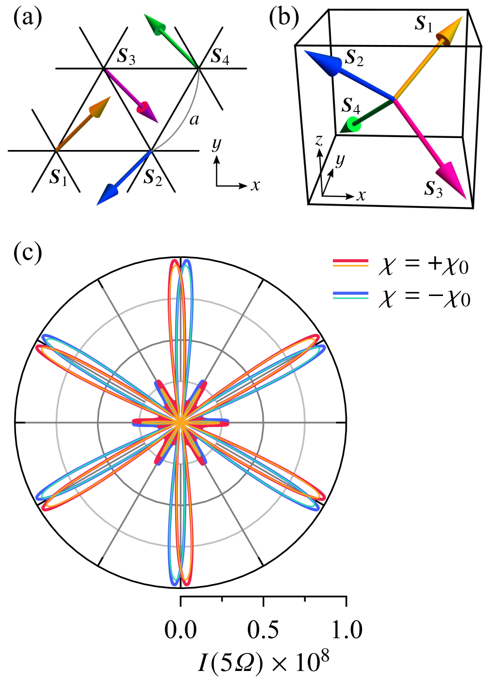

Figure 1: (a) Magnetic unit cell of the four-sublattice spin scalar chiral state, and (b) configuration of the four localized spin vectors. (c) Polarization angle dependence of the fifth harmonic intensity. These figures are adapted from Ref. [1].

References

[1] A. Ono, S. Okumura, S. Imai, and Y. Akagi: Phys. Rev. B **110**, 125111 (2024).

Ferromagnetism in $CeRh_6Ge_4$: A DFT+DMFT study

Junya OTSUKI
Research Institute for Interdisciplinary Science, Okayama University, Okayama 700-8530

$CeRh_6Ge_4$ is a cerium-based compound that exhibits a ferromagnetic transition at T_c = 2.5 K. It has attracted significant attention due to the observation of a ferromagnetic quantum critical point under pressure, and associated non-Fermi-liquid behavior. Central to understanding these phenomena is the nature of Ce $4f$ electrons—whether they are localized or itinerant—and the mechanism stabilizing the ferromagnetic order. We investigate the ferromagnetic order in $CeRh_6Ge_4$, applying a recently developed method that succeeded in reproducing the quadrupolar ordering in a prototypical material, CeB_6 [1].

We employ a combination of density functional theory (DFT) and dynamical mean-field theory (DMFT) to investigate the magnetic properties of $CeRh_6Ge_4$. We begin with DFT calculations assuming itinerant $4f$ electrons, then incorporate strong local Coulomb interactions through DMFT, yielding localized $4f$ electrons. These calculations were done using the open-source software `DCore` [2]. With the converged solution in DFT+DMFT, we calculate the momentum-dependent susceptibilities using the strong-coupling-limit (SCL) formula, which was derived by approximating the Bethe-Salpeter equation in the DMFT [3]. We used the FAT node of the system B to treat the system size (the division of the Brillouin zone) up to $24 \times 24 \times 42$.

The results for the momentum-dependent susceptibilities reveal that the nearest-neighbor exchange interaction along the c-axis forms ferromagnetic chains, while weaker and anisotropic interactions in the ab-plane align these chains [4]. The intersite interactions follow an RKKY-like decay and are spin-isotropic along the c-axis but spin-anisotropic within the plane. The calculated transition temperature $T_c \approx 3.2$ K is in reasonable agreement with experiment, though slightly overestimated due to mean-field nature of the DMFT.

This work successfully reproduces the ferromagnetic ground state of $CeRh_6Ge_4$ using a localized $4f$ electron model and elucidates the microscopic origin of the magnetic ordering via intersite exchange interactions. It provides compelling theoretical evidence for the localized nature of $4f$ electrons at ambient pressure and a new insight of weakly interacting ferromgnetic chains. These findings establish a fundamental basis for elucidating pressure-induced quantum criticality in $CeRh_6Ge_4$.

References

[1] J. Otsuki, K. Yoshimi, H. Shinaoka, H. O. Jeschke, Phys. Rev. B **110**, 035104 (2024).

[2] H. Shinaoka, J. Otsuki, M. Kawamura, N. Takemori, K. Yoshimi, SciPost Phys. **10**, 117 (2021).

[3] J. Otsuki, K. Yoshimi, H. Shinaoka, Y. Nomura, Phys. Rev. B **99**, 165134 (2019).

[4] S. Itokazu, A. Kirikoshi, H. O. Jeschke, J. Otsuki, in preparation.

Computational study on spin splitting and x-ray spectroscopy responses in altermagnets using DFT+DMFT method

Atsushi Hariki

Department of Physics and Electronics,

Osaka Metropolitan University, 1-1 Gakuen-cho, Naka-ku, Sakai, Osaka 599-8531, Japan

We conducted a computational study on several candidate altermagnets (MnTe, CrSb, and NiF_2), a newly emerging class of collinear magnets that exhibit time-reversal symmetry-breaking responses despite having a compensated magnetic moment. Using our in-house DFT+DMFT and Hartree-Fock codes, along with the large-scale parallel computing resources provided by ISSP, we analyzed their electronic band structures and computed their optical responses to circularly polarized light in the x-ray regime.

First, we calculated the circular dichroism (CD) in the resonant inelastic x-ray scattering (RIXS) spectra of MnTe using the DFT+DMFT method. By comparing our results with recent experimental data, we demonstrated that the angular dependence of the RIXS-CD signal can be used to distinguish between different domains of the altermagnetic order. Furthermore, based on numerical simulations in both the ordered and normal phases, we showed that the RIXS-CD signal can remain finite even in the normal phase. This effect originates from non-Hermiticity in the Kramers–Heisenberg RIXS cross section, caused by coupling to continuum states involved in the optical propagation during the RIXS process [1].

We also calculated the x-ray magnetic circular dichroism (XMCD) spectra for NiF_2 [2]. A key challenge in identifying altermagnetism is the influence of spin–orbit coupling, which can perturb the altermagnetic order by inducing a small ferromagnetic canting. Based on our numerical simulations, we proposed a method to separate the altermagnetic and ferromagnetic contributions in the experimental XMCD spectra.

In addition, we investigated the electronic structures of $R_3Ni_2O_7$ [3] and $PbCrO_3$ using the DFT+DMFT method.

References

[1] D. Takegami *et al*., arXiv:2502.10809.

[2] A. Hariki *et al*., accepted in npj Quantum Materials.

[3] D. Takegami *et al*., **111**, 165101 (2025).

An inequivalent dimer model to describe compensated ferrimagnetism in organic compounds: Electronic states explored

Akito Kobayashi[a], Kouki Nunota[a], Kazuyoshi Yoshimi[b], Kenichiro Hashimoto[c], and Takahiro Misawa[b]

[a]*Department of Physics, Nagoya University, Nagoya 464-8602*

[b]*Institute for Solid State Physics, University of Tokyo, Kashiwa, Chiba 277-8581, Japan*

[c]*Department of Advanced Materials Science, University of Tokyo, Kashiwa, Chiba 277-8561, Japan*

Traditionally, collinear antiferromagnets, characterized by antiparallel spin alignment, have been considered incapable of exhibiting unconventional transport phenomena, such as the generation of spin currents. However, recent theoretical advancements have unveiled the existence of intriguing antiferromagnetic materials, including altermagnets and compensated ferrimagnets, which demonstrate unique transport properties, such as the anomalous Hall effect and spin current generation [1, 2, 3].

Despite these findings, research on compensated ferrimagnetic materials has largely been confined to inorganic compounds, such as alloys, with limited progress in their practical implementation.

In this study, we introduce a straightforward approach to achieve compensated ferrimagnetism using organic compounds with dimer structures [4]. Specifically, we propose a simple design principle whereby compensated ferrimagnetic materials can be realized if an antiferromagnetic order emerges within organic compounds containing two distinct types of dimers (Fig. 1). We highlight the potential for compensated ferrimagnetism to be realized in the organic compound (EDO-TTF-I)$_2$ClO$_4$ through this mechanism [4].

Furthermore, a theoretical analysis of a two-dimensional inequivalent dimer model employing mean-field theory reveals a diverse range of electronic states, including band insulator/metal, antiferromagnetic insulator/metal, small-spin-splitting insulator/metal, half metal, and compensated ferrimagnetic insulator.

References

[1] M. Naka et al., Nat. Commun. **10**, 1, (2019)

[2] H. van Leuken et al., Phys. Rev. Lett. **74**, 1171 (1995)

[3] S. Semboshi et al., Sci. Rep. **12**, 10687 (2022)

[4] T. Kawamura et al., Phys. Rev. Lett. **132**, 156502 (2024)

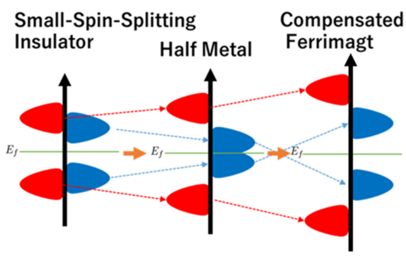

Figure 1: Diverse range of electronic states in the two-dimensional inequivalent dimer model

Quantum Damping of Magnons in Altermagnetism

Masahito MOCHIZUKI
Department of Applied Physics,
Waseda University, Okubo, Shinjuku-ku, Tokyo 169-8555

Altermagnetism is a newly identified class of nonrelativistic collinear magnetism that exhibits even-parity spin splitting, distinct from conventional ferromagnetism and antiferromagnetism. In this project (ID: 2024-Ba-0044), we study the stability of magnons against quantum many-body scatterings across all three classes of nonrelativistic collinear magnets [1].

Using kinematic analysis, nonlinear spin-wave (NLSW) perturbation theory, and density-matrix renormalization group with matrix-product-operator-based time evolutions (DMRG+tMPO), we demonstrate that magnon-magnon interactions universally destabilize the spin-split upper-branch magnons in altermagnets. In particular, in two-dimensional *d*-wave altermagnets, even an infinitesimal altermagnetic splitting opens up a decay phase space, leading to the emergence of a stable lower branch and an unstable upper branch in the long-wavelength limit. Furthermore, we show that NLSW perturbation theory with corrections up to the order $1/S^2$ (S being the spin length) accurately reproduces nonperturbative DMRG+tMPO results, highlighting spin-conserving three-magnon scattering processes [Fig. 1] as the leading quantum correction. We propose organic altermagnets as promising candidates for observing the predicted damped and long-lived magnons. This work sheds light on the potential for unique quantum spin dynamics in altermagnets.

In this project, parts of NLSW calculations are performed by using Ohtaka (System B).

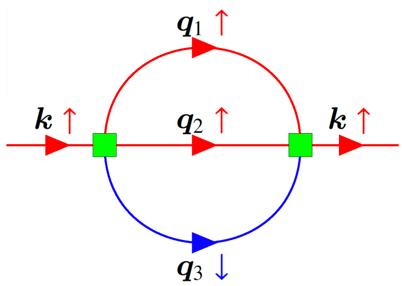

Fig. 1: Three-magnon forward bubble diagram with total spin conservation.

References

[1] R. Eto, M. Gohlke, J. Sinova, M. Mochizuki, A. L. Chernyshev, and A. Mook, preprint, arXiv:2502.20146

Theoretical study of enhancement mechanism of thermoelectric properties with spin fluctuations: A weak-coupling approach

Kazutaka NISHIGUCHI
Graduate School of System Informatics, Kobe University
Rokkodai-Cho, Nada-Ku, Kobe 657-8501

Ferromagnetic fluctuations in Heusler alloy Fe_2VAl

Heusler compound Fe_2VAl is one of the promising thermoelectric materials, which exhibits a large power factor $P = \sigma S^2$ with σ and S being the electrical conductivity and Seebeck coefficient, respectively. On the other hand, the thermal dimensionless figure of merit $ZT = \sigma S^2 T/\kappa$ is not so large yet reflecting its large thermal conductivity κ. Recently, it is experimentally observed in doped Fe_2VAl (i.e., $Fe_2V_{0.9}Cr_{0.1}Al_{0.9}Si_{0.1}$ and $Fe_{2.2}V_{0.8}Al_{1-y}Si_y$) as a weekly ferromagnetic material that ferromagnetic fluctuations enhance the thermoelectric properties such as S and P around the Curie temperature ($T_c = 285$ K). [1] It is not only a desirable property for practical use in realistic (room) temperatures, but also a fundamental and intriguing quantum phenomena where quantum fluctuations and thermoelectric effects are entangled by electron correlations.

Motivated above, we have studied electronic properties of Fe_2VAl using first-principles calculations based on the density functional theory (DFT) within the generalized gradient approximation (GGA). We performed DFT calculations with the Perdew–Burke–Ernzerhof (PBE) exchange-correlation functional for solids (PBEsol) and the projector augmented wave (PAW) method using The Vienna Ab Initio Simulation Package (VASP) [2] and Quantum ESPRESSO (QE) package. [3]

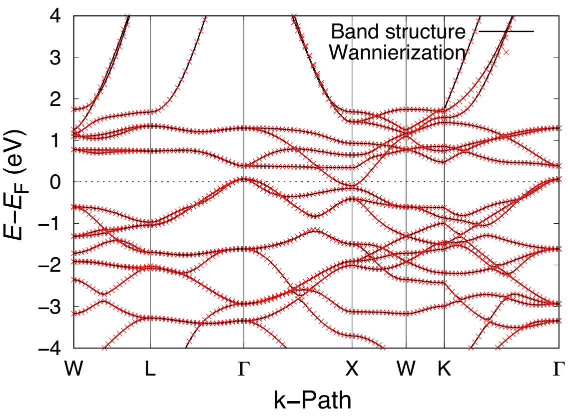

Figure 1: DFT band structure and Wannierization of Fe_2VAl.

Using the maximally localized Wannier functions, we could construct a low-energy effective model from the first- principles bands around the Fermi level. The effective model is composed of the Fe-3d, V-3d, and Al-2sp3 Wannier orbitals, namely, 19 orbitals. The DFT and structure and Wannier orbitals are shown in Fig. 1.

Furthermore, the obtained 19-orbital effective model was investigated using the random phase approximation (RPA). The susceptibilities show that the spin fluctuations are dominant compared to the charge ones. Also, the obtained spin susceptibility has a peak at $q = (0, 0, 0)$, which reflects the ferromagnetic instability. This is consistent with the fact that Fe_2VAl exhibits the weak ferromagnetism.

Calculation conditions

We have performed the DFT calculations using the hybrid (MPI+OpenMP) parallel computing, where the parallelization over bands and k-points is used by VASP version 6.4.2 and QE version 7.2.

References

[1] N. Tsujii, A. Nishide, J. Hayakawa, and T. Mori: Sci. Adv. **5**, eaat5935 (2019).

[2] G. Kresse *et. al.*: Phys. Rev. B **47**, 558 (1993); Phys. Rev. B **49**, 14251 (1994); Computational Materials Science **6** (1996) 15–50; Phys. Rev. B **54**, 11169 (1996).

[3] P. Giannozzi *et. al.*: J. Phys.: Condens. Matter **21**, 395502 (2009) ; J. Phys.: Condens. Matter **29**, 465901 (2017) ; J. Chem. Phys. **152**, 154105 (2020).

[4] I. Souza, N. Marzari, and D. Vanderbilt: Phys. Rev. B **65**, 035109 (2001) ; A. A. Mostofi *et. al.*: Comput. Phys. Commun. **178** (2008) 685–699; A. A. Mostofi *et. al.*: Comput. Phys. Commun. **185** (2014) 2309–2310; G. Pizzi *et. al.*: J. Phys.: Condens. Matter **32**, 165902 (2020).

Theoretical study of BCS-BEC crossover in strongly correlated electron systems

Hiroshi WATANABE
Department of Liberal Arts and Basic Sciences, College of Industrial Technology, Nihon University
2-11-1 Shin-ei, Narashino, Chiba 275-8576

The BCS-BEC crossover, which smoothly connects Bardeen-Cooper-Schrieffer (BCS) theory with Bose-Einstein condensation (BEC), has attracted significant attention across various fields as a fascinating quantum phenomenon. Recently, in addition to ultracold Fermi gases, the possibility of a BCS-BEC crossover has been discussed in strongly correlated electron systems including the iron-based superconductors, the two-dimensional organic superconductor κ-(ET)$_4$Hg$_{2.89}$Br$_8$ (κ-HgBr) [1], and cuprate superconductors. However, identifying the BCS-BEC crossover in such systems is far more challenging than in Fermi gases due to unconventional (non-s-wave) gap symmetry and competition with various magnetic and/or charge orders. Understanding the crossover in this context may offer valuable insights into unconventional pairing mechanism and the interplay with competing quantum phases.

The organic superconductor κ-HgBr is a promising candidate due to its doped spin-liquid-like nature and tunable electron correlations. In this study, we investigate the extended Hubbard model on an anisotropic triangular lattice using the variational Monte Carlo method and discuss the possibility of the BCS-BEC crossover in κ-type organic superconductors [2]. The system size for the calculation is N=24×24=576 unit cells (and thus 576×2=1152 molecules in total) and the calculation has been carried out mainly using system B at the ISSP Supercomputer Center. To enable such large-scale simulations, we employed MPI parallelization, which significantly enhanced computational efficiency and made the extensive parameter space exploration feasible.

As shown in Fig. 1, for hole doping rate δ=0.06, the superconducting correlation function $P_{\rm SC}$ exhibits a dome-shaped dependence on interaction strength U/t, which is a hallmark of the BCS-BEC crossover. Other physical quantities including the superfluid weight, the coherence length, and the chemical potential also display characteristic changes. In contrast, for δ=0 or 0.11, the system undergoes transitions to a Mott insulator or stripe-ordered phase, respectively, and superconductivity is suppressed.

Our results demonstrate that the BCS-BEC crossover can emerge when competing phases are suppressed through appropriate hole doping. These findings provide a clear theoretical criterion for identifying the BCS-BEC crossover in real materials and suggest experimental strategies to realize it in strongly correlated electron systems.

References

[1] Y. Suzuki *et al.*, Phys. Rev. X **12**, 011016 (2022).

[2] H. Watanabe and H. Ikeda, Phys. Rev. B **111**, 085130 (2025).

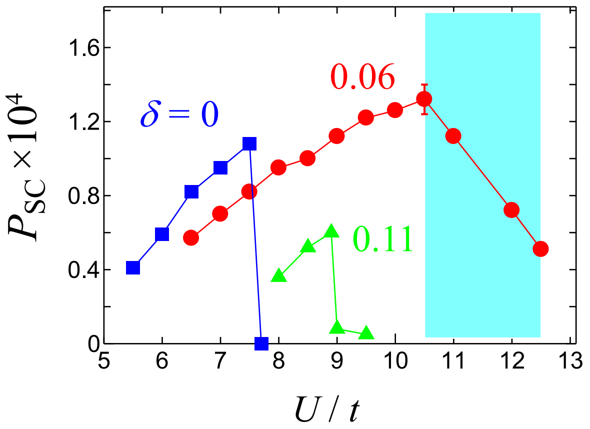

Figure 1: U/t dependence of the superconducting correlation function P_{SC} for the hole doping rate $\delta = 0$, 0.06, and 0.11 [2].